

Dedicated to Professor Dr. ALEXANDRU T.
BALABAN, member of the Roumanian Academy
on the occasion of his 75th anniversary

QSAR ANALYSIS OF A SERIES OF IMIDAZOLE DERIVATIVES ACTING ON THE H₃ RECEPTOR

Maria MRACEC,* Laura JUCHEL and Mircea MRACEC

Roumanian Academy, Institute of Chemistry “Coriolan Drăgulescu” Timișoara,
Bd. Mihai Viteazul 24, RO-300223 Timișoara, Roumania,
mmracec@acad-icht.tm.edu.ro

Received November 18, 2005

A classical QSAR analysis was performed on a series of 29 imidazolic derivatives acting as histamine antagonists at the H₃ receptor. Steric descriptors (solvent accessible surface area, van der Waals area and volume), electronic descriptors (AM1 polarizability, energy of frontier orbitals, dipole moment) hydrophobicity descriptors (logP) and constitutional descriptors were tested in multiple linear regressions. Many models with high statistical significance were obtained applying the MTD method. These models contain as descriptors MTD, hydration energy, LUMO energy, logP, heat of formation and solvent accessible surface area, descriptors that support the importance of steric interactions with H₃ receptor. The minimum topological difference, MTD descriptor together with hydration energy and molecular mass, Mr give a model with predictive value ($r^2 = 0.880$, $see = 0.181$, $F = 60.89$, $r^2_{CV} = 0.667$, $press = 2.28$). The model was validated by calculating the activity of four compounds not included in the training series. The optimized receptor map corresponding to this model suggests that branching at two carbon atoms of the alkyl chain is detrimental for the antihistaminic activity.

INTRODUCTION

Antagonists of histamine acting on the H₃ receptors have potential therapeutic applications in different CNS diseases: depression,¹ bulimia,² epilepsy,^{3,4} schizophrenia, insomnia, sleeping disease, Alzheimer's syndrome, temporary loss of memory and incapacity of learning.⁵⁻⁹ Presently, many active H₃ antagonists are known as for example thioperamide and clobenpropit. Unfortunately, these compounds contain hepatotoxic groups of thiourea or isothiourea and for this reason they were not introduced in clinical trials. Searching for less toxic compounds with high activity and selectivity on the H₃ receptor, Schunack *et al.*¹⁰ synthesized compounds similar to clobenpropit containing carbamate group instead of thiourea. We used these experimental data in a classical QSAR study to evidence the physico-chemical properties important for the high activity of histamine antagonists acting on the H₃ receptor.

METHODS

Gas phase equilibrium geometry of the compounds was obtained using a molecular mechanics method, the MM+ force field, and a semiempirical quantum chemical method, AM1 Hamiltonian, from HyperChem7.0 package (demo version). In order to obtain the conformer in the lowest minimum on the potential energy surface, a conformational analysis was performed using the MM+ force field and the Conformational Search module from HyperChem7.0. An energy criterion of 10 kcal/mol above the best conformer was used. Maximum number of optimization cycles was set to 3000 and the lowest 100 conformers above the best conformer were kept. All conformers resulted from conformational search were further optimized using the semiempirical quantum chemical method AM1. Geometry optimizations were

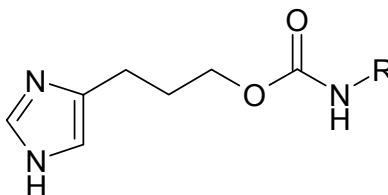
performed with the Polak-Ribiere conjugate gradient algorithm. SCF convergence was set at 10^{-5} and the RMS gradient at 0.01 kcal/Åmol. For racemates two series of geometries, containing either (R) chiral atoms or (S) chiral atoms, were optimized.

Using the MM+ optimized geometry a set of descriptors were calculated: total energy, stretching energy, E_{stretch} , bending energy, E_{bend} , torsion energy, E_{tors} , and van der Waals energy, E_{VDW} and used as descriptors in correlation with pKi (reciprocal logarithm of inhibition constant–molar concentration). The AM1 optimized geometry was used to calculate a number of electronic descriptors: dipole moment, DM, sp hybridization component of dipole moment, DM_{hyb} , energy of frontier orbitals, E_{HOMO} and E_{LUMO} , net charges on the N atom from the carbamate group and its neighbour carbon atoms of substituents and heat of formation. Using the QSAR properties module from HyperChem7.0 polarizability, α , molar refractivity, MR, logP (partition coefficient octanol/water), hydration energy, E_{Hy} , van der Waals area, A_{VDW} , and volume, V_{VDW} , solvent accessible surface area, A_{SAS} , solvent-accessible surface-bounded molecular volume, V_{SAS} were calculated. Some constitutional and topological descriptors were calculated with the DRAGON program.

The MTD method¹¹ was applied to calculate the minimum topological difference (MTD) descriptor. Structure and biological activities¹⁰ for a series of 29 imidazolic derivatives acting on the H₃ receptor are presented in Table 1.

Table 1

Structure, antihistaminic activity, pKi, and occupancy of hypermolecule vertices



No.	R	pK _i	occupancy, $\varepsilon_i(x_{ij}=1)$	MTD1	MTD2
1	CH ₂ -CH ₃	6.5	1, 2	7	4
2	CH(CH ₃) ₂	7.09	1, 2, 13	7	5
3	(CH ₂) ₂ -CH ₃	7.35	1-3	6	4
4	(R/S)-CH(CH ₃)CH ₂ -CH ₃	7.7	1-3, 13	6	5
5	(R)-CH(CH ₃)CH ₂ -CH ₃	7.72	1-3, 14	5	5
6	(S)-CH(CH ₃)CH ₂ -CH ₃	7.64	1-3, 13	5	6
7	CH ₂ -CH(CH ₃) ₂	7.52	1-3, 15	6	5
8	(CH ₂) ₃ -CH ₃	7.77	1-4	5	3
9	(R/S)-CH(CH ₃)(CH ₂) ₂ -CH ₃	7.6	1-3, 13	6	5
10	(R)-CH(CH ₃)(CH ₂) ₂ -CH ₃	7.92	1-4, 14	5	4
11	(R/S)-CH ₂ -CH(CH ₃)CH ₂ -CH ₃	7.85	1-4, 15	5	4
12	(S)-CH ₂ -CH(CH ₃)CH ₂ -CH ₃	7.74	1-4, 15	5	6
13	(CH ₂) ₂ -CH(CH ₃) ₂	8.19	1-4, 11	5	4
14	(CH ₂) ₄ -CH ₃	8.07	1-4, 8	4	3
15	(CH ₂) ₃ -O-CH ₃	6.81	1-4, 8	5	4
16	(CH ₂) ₃ -S-CH ₃	7.66	1-4, 8	5	4
17	(R/S)-CH(CH ₃)(CH ₂) ₃ -CH ₃	8.06	1-4, 8, 13	5	5
18	(R)-CH(CH ₃)(CH ₂) ₃ -CH ₃	7.72	1-4, 8, 14	6	5
19	(S)-CH(CH ₃)(CH ₂) ₃ -CH ₃	7.92	1-4, 8, 13	5	5
20	(R/S)-CH ₂ -CH(CH ₃)(CH ₂) ₂ -CH ₃	7.82	1-4, 8, 15	5	5
21	(R/S)-(CH ₂) ₂ -CH(CH ₃)CH ₂ -CH ₃	8.29	1-4, 8, 11	4	4
22	(CH ₂) ₅ -CH ₃	8.07	1-4, 8, 9	5	5
23	(R/S)-CH(CH ₃)(CH ₂) ₄ -CH ₃	7.74	1-4, 8, 9, 13	4	6
24	(R)-CH(CH ₃)(CH ₂) ₄ -CH ₃	7.64	1-4, 8, 9, 14	6	5
25	(S)-CH(CH ₃)(CH ₂) ₄ -CH ₃	7.74	1-4, 8, 9, 13	5	4
26	(CH ₂) ₆ -CH ₃	8.39	1-4, 8-10	4	5
27	(R/S)-CH(CH ₃)(CH ₂) ₅ -CH ₃	7.74	1-4, 8-10, 13	5	6
28	(CH ₂) ₇ -CH ₃	8.29	1-4, 8-10, 12	4	5
29	Clobenpropit	9.22	1-7	2	0

ε_i = occupancy of vertices in hypermolecule in Fig 1; MTD1 = MTD optimized without partner descriptors; MTD2 = MTD optimized with hydration energy, E_{Hy} and molecular mass, Mr.

RESULTS

The hypermolecule for this series has 15 vertices. The numbering of vertices is shown in Fig 1. Occupancy of the hypermolecule vertices by the atoms of each molecule from the series is displayed in Table 1.

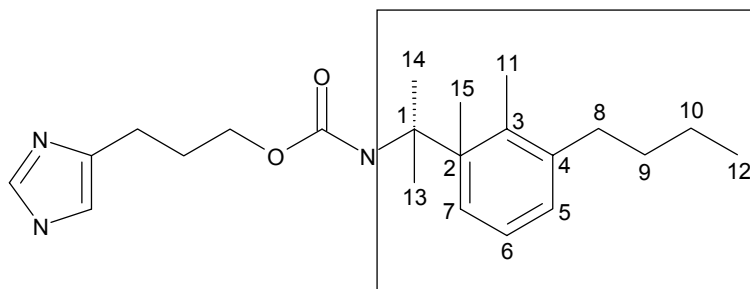


Fig. 1 – Hypermolecule (enclosed in the rectangle) and numbering of its vertices.

Statistical data for some regressions with statistic significance are shown in Table 2. Regressions were obtained with compounds having carbon atoms with S chirality. The results for the series of compounds with R chirality do not differ significantly.

Table 2

Statistical values of some monoparametric regressions after elimination of outliers

Descriptors	r	s	F	n	Outliers
P _{ZZ}	0.769	0.257	34.71	26	1,15,21
A _{SAS}	0.628	0.316	15.84	27	15,29
V _{SAS}	0.648	0.297	18.15	27	15,29
E _{Hy}	0.659	0.266	19.28	27	1,29
A _{VDW}	0.664	0.292	19.72	27	15,29
logP	0.668	0.263	20.16	27	1,29
clogP	0.686	0.257	22.21	27	1,29
V _{VDW}	0.671	0.289	20.55	27	15,29
MW	0.755	0.311	34.41	28	15
Mr	0.68	0.236	79.16	28	15
P _{YY}	0.701	0.359	26.15	29	-
MTD	0.828	0.282	58.87	29	-

P_{ZZ}, P_{YY} – polarizability components (AM1); A_{SAS} – solvent accessible area; V_{SAS} – solvent-accessible surface-bounded molecular volume; E_{Hy} – hydration energy; A_{VDW} and V_{VDW} – van der Waals area and volume; Mr – molecular mass given in ref 10; logP(HyperChem) and clogP – octanol-water partition coefficients; MW – molecular weight; MTD – minimum topological difference

For calculating the MTD descriptor, the initial receptor map for the S series (see Fig 1) was:

$$S^0 \begin{cases} \varepsilon_j = -1: & 1 - 7 \\ \varepsilon_j = 0: & 8 - 12 \\ \varepsilon_j = 1: & 13 - 15 \end{cases}$$

The following optimized receptor map without detrimental vertices resulted:

$$S^1 \begin{cases} \varepsilon_j = -1: & 1 - 7, 10, 11 \\ \varepsilon_j = 0: & 8, 9, 12 - 15 \\ \varepsilon_j = 1: & - \end{cases}$$

The corresponding regression was:

$$pK_i = 9.8411(0.2827) - 0.4056(0.0548) \text{ MTD} \quad (1)$$

$$n = 29 \quad r^2 = 0.670 \quad r^2_{\text{adj}} = 0.658 \quad s = 0.289 \quad F = 54.85 \quad r^2_{\text{CV}} = 0.464 \quad \text{press} = 3.67$$

Starting from the same initial receptor map another optimized receptor map was obtained for descriptors MTD, E_{Hy} , Mr. It contains 5 detrimental vertices. Three of them 13-15 are due to the aliphatic branching.

$$S^2 \begin{cases} \varepsilon_j = -1: & 1, 2, 4 - 7 \\ \varepsilon_j = 0: & 3, 10 - 12 \\ \varepsilon_j = 1: & 8, 9, 13 - 15 \end{cases}$$

The corresponding regression was:

$$pK_i = 8.4156 (0.5960) + 0.2726 (0.0417) E_{\text{Hy}} + 0.0076 (0.0007) \text{ Mr} - 0.2752 (0.0459) \text{ MTD} \quad (2)$$

$$n = 29 \quad r^2 = 0.880 \quad r^2_{\text{adj}} = 0.865 \quad s = 0.181 \quad F = 60.89 \quad r^2_{\text{CV}} = 0.667 \quad \text{press} = 2.28$$

In Table 3 cross-correlation coefficients are shown. The MTD descriptor correlates strongly with E_{Hy} . This suggests that the MTD descriptor contains information related to conformational stability.

Table 3

Cross-correlation coefficients for descriptors from model (2)

	Mr	E_{Hy}	MTD	pKi
Mr	1.000	-0.236	-0.331	0.812
E_{Hy}		1.000	0.760	0.017
MTD			1.000	-0.381

By introducing other descriptors in model (2), as for example A_{SAS} , E_{LUMO} , the multiple correlation coefficient slightly increased but the cross-validated correlation coefficient had values lower than 0.667, the value from model (2). In Table 4 are presented the pKi values calculated with models (1) and (2).

Table 4

pKi values calculated with models (1) and (2) and differences between observed and calculated pKi values

Obs	Ec. (1)		Ec. (2)	
	Calc	Diff	Calc	Diff
6.5	7.002	-0.502	6.364	0.136
7.09	7.002	0.088	7.227	-0.137
7.35	7.408	-0.058	7.544	-0.194
7.7	7.408	0.292	7.425	0.275
7.72	7.813	-0.093	7.844	-0.124
7.64	7.813	-0.173	7.778	-0.138
7.52	7.408	0.112	7.430	0.090
7.77	7.813	-0.043	8.040	-0.270
7.6	7.408	0.192	7.668	-0.068
7.92	7.813	0.107	7.909	0.011
7.85	7.813	0.037	7.957	-0.107
7.74	7.813	-0.073	7.871	-0.131

(continues)

Table 4 (continued)

8.19	7.813	0.377	7.870	0.320
8.07	8.219	-0.149	8.246	-0.176
6.81	7.813	-1.003	7.039	-0.229
7.66	7.813	-0.153	7.580	0.080
8.06	7.813	0.247	7.841	0.219
7.72	7.408	0.312	7.588	0.132
7.92	7.813	0.107	7.934	-0.014
7.82	7.813	0.007	7.844	-0.024
8.29	8.219	0.071	8.119	0.171
8.07	7.813	0.257	7.897	0.173
7.74	8.219	-0.479	7.983	-0.243
7.64	7.408	0.232	7.654	-0.014
7.74	7.813	-0.073	7.898	-0.158
8.39	8.219	0.171	8.053	0.337
7.74	7.813	-0.073	7.776	-0.036
8.29	8.219	0.071	8.235	0.055
9.22	9.030	0.190	9.157	0.063
$\Sigma(\text{obs-pred})^2$		2.256		0.823

Introduction of the E_{Hy} and Mr descriptors increases significantly the values of r^2 , r^2_{cv} and decreases significantly $\Sigma(\text{obs-pred})^2$. The optimized receptor map corresponding to model (2) is different from that obtained from MTD optimized without partner descriptors. In model (2) vertex 3 gives correlation coefficients closer to a beneficial vertex than to a detrimental one, while vertex 10 is closer to a detrimental vertex than to a beneficial vertex. The optimized receptor map for model (2) suggests that the receptor pocket gives unfavorable sterical interactions with compounds containing branching at vertices 1 or 2.

Predictability of model (2) was tested for other four derivatives not included in this series. Structure, values of descriptors and experimental and predicted biological activities obtained with model (2) are shown in Table 5.

Table 5

Structure, descriptor values, experimental and predicted pKi and difference between them							
	R	Mr	E_{Hy}	MTD	pKi (exp)	pKi (pred)	Diff
I	Ph	379.9	-10.72	0	7.959	8.370	-0.411
II	4-NH ₂ -Ph	394.9	-14.82	1	6.267	7.090	-0.823
III	2-furyl	369.8	-12.50	1	7.377	7.534	-0.157
IV	2-thienyl	385.9	-11.32	1	7.745	7.976	-0.231

Compound II has the NH₂ group occupying a vertex not considered in the hypermolecule and its pKi value is under the minimum value for this series, namely lower than 6.5. This could explain the large difference between experimental and predicted value given by model (2).

CONCLUSIONS

In the series of imidazolic ligands many descriptors correlate with the antihistaminic activity. pKi is influenced by steric descriptors (MTD, areas, volumes), electronic descriptors (polarizability) and hydrofobicity (logP, clogP). Although many physico-chemical descriptors correlate with the antihistaminic activity, they strongly cross-correlate to each other and the resulted regressions cannot be reliably interpreted.

No statistically significant difference resulted between the correlations of the (S) chiral series and of the (R) chiral series suggesting that the H₃ receptor is not specifically stereo-selective toward the imidazolic ligands in this series. Branching of the substituent at the carbon atom bound to the amidic group as well as branching at the next carbon atom of the substituent is detrimental to the antihistaminic activity.

REFERENCES

1. C. Perez-Garcia, L. Morales, M.V. Cano, I. Sancho and L.F. Alguacil, *Psychopharmacology (Berl.)*, **1999**, *142*, 215-20.
2. K. Takahashi, H. Suwa, T. Ishikawa and H. Kotani., *J. Clin. Invest.*, **2002**, *110*, 1791-1799.
3. M.B. Passani and P. Blandina, *Methods Find Exp. Clin. Pharmacol.*, **1998**, *20*, 725-33.
4. H. Stark, E. Schlicker and W. Schunack, *Drugs Future*, **1996**, *21*, 507-20.
5. J.C. Schwartz, J.M. Arrang, M. Garbarg, H. Pollard and M. Ruat, *Physiol. Rev.*, **1991**, *71*, 1-51.
6. R. Leurs, M. Kathmann, R.C. Vollinga, W.M.P.B. Menge, E. Schlicker and H. Timmerman, *J. Pharmacol. Exp. Ther.*, **1996**, *276*, 1009-1015.
7. J.C. Schwartz, S. Morisset, A. Rouleau, X. Ligneau, F. Gbahou, J. Tardivel-Lacombe, H. Stark, W. Schunack, C.R. Ganellin and J.M. Arrang, *J. Neural Transm. Suppl.*, **2003**, *64*, 1-16.
8. H. Stark, M. Kathmann, E. Schlicker, W. Schunack, B. Schlegel and W. Sippl, *Mini Rev. Med. Chem.*, **2004**, *4*, 965-77.
9. W. Schunack and H. Stark, *Eur. J. Drug Metab. Pharmacokinet.*, **1994**, *19*, 173-8.
10. A. Sasse, K. Kiec-Kononowicz, H. Stark, M. Motyl, S. Reidemeister, C.R. Ganellin, X. Ligneau, J.C. Schwartz, W. Schunack and *J. Med. Chem.*, **1999**, *42*, 593-600.
11. Z. Simon, *MTD and hyperstructure approaches*. In *3D-QSAR in Drug Design Theory, Methods, Applications*, H. Kubiny, Ed. ESCOM Leyden, 1993, p. 307-319.
12. M.J.S.Dewar, E.G. Zoebish, E.F. Healy and J.J. Stewart, *J. Am. Chem. Soc.*, **1985**, *107*, 3902-3909.